Solid Phase Extraction Penicillin and Tetracycline in Human Serum Using Magnetic Graphene Oxide-Based Sulfide Nanocomposite

Hassan Sereshti [1], Sara Soltani [1], Nanthini Sridewi [2,*], Elham Salehi [3], Ehsan Parandi [4], Hamid Rashid Nodeh [3] and Syed Shahabuddin [5,6,*]

1   School of Chemistry, College of Science, University of Tehran, Tehran 1417614411, Iran
2   Department of Maritime Science and Technology, Faculty of Defence Science and Technology, National Defence University of Malaysia, Kuala Lumpur 57000, Malaysia
3   Food Technology and Agricultural Products Research Center, Standard Research Institute, Karaj 3174734563, Iran
4   Department of Food Science & Technology, Faculty of Agricultural Engineering and Technology, University of Tehran, Karaj 6719418314, Iran
5   Department of Chemistry, School of Energy Technology, Pandit Deendayal Energy University, Raisan, Gandhinagar 382426, Gujarat, India
6   Faculty of Applied Sciences, Universiti Teknologi MARA, Cawangan Negeri Sembilan, Kampus Kuala Pilah, Kuala Pilah, Shah Alam 40450, Malaysia
*   Correspondence: nanthini@upnm.edu.my (N.S.); syedshahab.hyd@gmail.com or syed.shahabuddin@sot.pdpu.ac.in (S.S.); Tel.: +60-124-675-320 (N.S.); +91-858-593-2338 (S.S.)

Abstract: Herein, we report a procedure for separating and preconcentrating antibiotics from human serum using a novel adsorbent of magnetic graphene oxide (MGO) and cadmium sulfide (CdS) nanoparticles. The adsorbent (MGO@CdS) was characterized using Fourier transformed infrared spectrometry (FT-IR), energy dispersive X-ray spectroscopy (EDX), and field emission scanning electron microscopy (FE-SEM). The effective parameters for extraction efficiency were investigated, including the desorption solvent's nature, pH, adsorbent dose, salt concentration, extraction time, and volume of sample solution and desorption solvent. The proposed procedure proved to be fast (20 min), simple (two stages), and cost-effective (20 mg of nanoparticles). Under the optimum conditions, satisfactory linearity ($R^2 > 0.992$) was obtained, and limits of detection (LOD) were estimated as 4.5 µg L^{-1} (for tetracycline) and 5.7 µg L^{-1} (for penicillin) and a linear dynamic range (LDR) from 20 to 200 µg L^{-1}. The magnetic solid phase extraction (MSPE) method based on MGO@CdS has achieved a satisfactory recovery (71.5–109.5%) in human serum for the selected antibiotics. Finally, the antibiotic's release was studied in simulated fluids of the gastric (pH = 1.2) and intestine (pH = 7.4). In this light, we demonstrate that the newly introduced adsorbent can be used in drug extraction from different biological media.

Keywords: magnetic solid phase extraction; cadmium sulfide nanoparticles; penicillin; tetracycline; biological serum samples

1. Introduction

In recent years, there has been growing concern about the presence of pharmaceutical residues in various biological mediums and water resources worldwide [1]. Antibiotics, a class of drugs with powerful antibacterial capabilities, are commonly used to treat bacterial infections in humans and animals [2]. Antibiotics, which also include tetracyclines and penicillin, are among the medications that are most commonly utilized for the treatment of diseases that are caused by bacteria [3]. Tetracycline is widely used with beneficial properties such as low adverse side effects, low toxicity, a relatively low price, few allergic indications, and a high therapeutic index [4]. Thus, the US Center for Disease Control

and Prevention reported that approximately 23,000 Americans die annually of antibiotic-resistant infections [5]. One of the other extensively used antibiotics is penicillin, which was discovered by Alexander Fleming in 1928 and was a breakout event in medicine [6]. This drug inhibits the cross-linkage of an amino sugar in gram-negative and positive bacterial cell walls when it is bound to the transpeptidase domain of penicillin binding proteins (PBPs), leading to the cell's death [7]. To prevent the development of such resistance in the human body, it is necessary to monitor the penicillin dose in the blood. Therefore, it is essential to determine the tetracycline and penicillin antibiotics in biological samples, which is the purpose of this work.

Some useful methods for determining antibiotics include biosensors with great sensitivity and repeatability [8]. However, sample preparation is required before instrument analysis due to the complex matrices of biological samples (i.e., blood, plasma, saliva, and urine) and to decrease the interference effects [9]. Several analytical methods based on liquid and solid phase extractions (SPE) have been developed to extract and pre-concentrate the analytes in biological samples. Liquid-liquid extraction (LLE) was the pioneering method of sample preparation in analytical chemistry. Its primary drawbacks are its effective use of organic solvent and several iterations of the extraction process. Because of this, solid phase extraction (SPE) emerged as a viable replacement for LLE because it is one of the most widespread sample treatments employed as a cleanup and preconcentration step [10]. SPE is the most common technique in sample preparation [11,12], due to its wide variation of sorbents, flexibility, high enrichment factor, noticeable extraction recovery, good sensitivity, selectivity, and reusability [6]. Although conventional SPE has gained potential benefits, it is tedious and time-consuming, especially when loading a high sample volume and requiring a low breakthrough volume [13]. However, the main drawbacks of "traditional" SPE are the high backpressure generated and the elevated amount of sorbent necessary. As an alternative, other approaches such as solid phase microextraction (SPME), dispersive solid phase extraction (DSPE), dispersive solid phase microextraction (DSPME), and magnetic solid phase extraction (MSPE) have been described. Hence, to overcome the limitations of SPE, magnetic nanoparticles (MNPs) were doped on solid materials to improve the SPE procedure and make it a simple and fast extraction method [14]. Thus, with the presence of MNPs and the application of an external magnet in MSPE, the tedious cartridge packing, filtration, and centrifuging processes are avoided. In addition, ease, convenience of use [15], and high enrichment factor and extraction efficiency values are other benefits of MSPE [16]. The Fe_3O_4 MNPs are the most common sorbents in MSPE since they contain a high surface area, quite small particles, excellent paramagnetic properties, water dispersity, stability, and less toxicity [17]. Moreover, they are easy to synthesize and functionalize, as well as applicable in biological samples. Nevertheless, to increase the adsorption capacity and sensitivity, further modification of Fe_3O_4 MNPs is essential.

Due to their high adsorption capacity for organic molecules, C18, fullerenes, carbon nanobers, carbon nanotubes, and graphene, as well as their functionalized forms, have recently been explored as adsorbent materials in MSPE methods [18]. Among them, graphene oxide is a new allotrope of carbon that is widely used as an MSPE sorbent [19]. Graphene oxide as a low-cost adsorbent provides fascinating properties, including a high specific surface area ($2630 \text{ m}^2 \text{ g}^{-1}$) [6], admirable thermal conductivity, considerable mechanical strength, and a free-standing two-dimensional mono-layer sheet of carbon atoms with a honeycomb structure [19]. The powerful techniques, namely X-ray photoelectron spectroscopy (XPS), 13C-NMR, and Raman spectroscopy, demonstrated the presence of various functional groups, such as lactol, epoxy (as bridges), hydroxyl group, and carboxyl group, on graphene oxide individual planes and the edges [16]. Furthermore, functional groups establish covalent and non-covalent interactions, such as hydrogen binding [6], hydrophilic interaction, π-π stacking, and electrostatic interaction [6], with various analytes. In addition, GO is chemically stable enough, even with hydroxyl radicals, making GO composites with macroscopic structure a suitable candidate for long-lived recyclable adsorbents for the enrichment of carbon-based ring structures [18]. Incorporating CdS

with graphene oxide (GO) enhances its efficiency due to its effective adsorption properties and high electron mobility with a greater surface area [20]. Cherkashina, Voznesenskiy, Osmolovskaya, Vakh, and Bulatov [3] used surfactant-coated Fe_3O_4 magnetic nanoparticles to separate and preconcentrate tetracycline from human serum samples using magnetic dispersive micro-solid phase extraction. They reported that the analytical curves were linear in the ranges of 0.25–10 mg L^{-1} for tetracycline using relatively small amounts of nanoparticles (10 mg). Xu et al. [21] also determined tetracycline residues in miniaturized SPE Using chitosan-modified graphitized multiwalled carbon nanotubes. They reported $R^2 > 0.992$ of linearity and a LOD range of $0.61-10.34$ µg/kg. They showed that the mean recoveries of the 5 tetracycline antibiotic residues in the real samples were between 81.5 and 101.4%. Wang et al. [22] showed satisfied linearity in the range of 4–70 ng mL^{-1} and LOD (0.6–3 ng mL^{-1}) and LOQ (2 to 10 ng mL^{-1}) for covalent organic frameworks. COF-SCU1 incorporated electrospun nanofibers as adsorbent in pipette tip solid-phase extraction (PT-SPE) of tetracycline antibiotics.

To the best of our knowledge, there is no report about the use of MGO@CdS as a sufficient adsorbent in the SPE of antibiotics. In the current study, a novel nanocomposite was synthesized by doping CdS nanoparticles on the surface of magnetic graphene oxide to produce MGO@CdS. This nanocomposite was successfully applied for the preconcentration of penicillin and tetracycline from a biological sample (human plasma). The MGO@CdS has gained high extraction recovery value for selected antibiotics since graphene can form π-π interactions with the benzene rings of analytes. Additionally, graphene prevents CdS nanoparticles from aggregation; consequently, a smaller particle size was achieved. Furthermore, CdS nanoparticles have increased the extraction performance through different electrostatic interactions and H-bonding with analytes. Finally, drug delivery approaches of MGO@CdS were evaluated for penicillin and tetracycline in simulated fluids of the gastric (pH = 1.2) and intestine (pH = 7.4).

2. Materials and Methods

2.1. Materials and Chemicals

Graphite, iron (II) chloride tetrahydrate ($FeCl_2 \cdot 4H_2O$), iron (III) chloride hexahydrate ($FeCl_3 \cdot 6HO$), sodium hydroxide (NaOH), polyethene glycol (PEG), cadmium acetate dehydrate ($Cd(CH_3COO)_2 \cdot 2H_2O$), methanol ($CH_3OH$), sodium thiosulfate pentahydrate ($Na_2S_2O_3 \cdot 5H_2O$), hydrochloride acid (HCl), nitric acid (HNO_3) 65%, and sulfuric acid (H_2SO_4) 97% were analytical grade and purchased from Merck Chemicals (Darmstadt, Germany). The pharmaceutical standards of tetracycline and penicillin were bought from Solarbio Science & Technology Co., Ltd. (Beijing, China). Human serum (pooled from male AB plasma) was procured from Sigma (H4522, Sigma-Aldrich Corporation, St. Louis, MO, USA).

2.2. Instruments

The morphology and chemical structure of the synthesized adsorbent were studied by field-emission scanning electron microscopy and energy-dispersive X-ray spectroscopy (FE-SEM/EDX) at TESCAN MIRA3 (Brno, Czech Republic). The FT-IR spectra were obtained in the range of 450–4000 cm^{-1} using KBr pellets and a Bruker EQUINOX 55 FTIR spectrometer (Bremen, Germany). The UV-vis absorption spectra were recorded on a RAYLEIGH UV-2601 (Beijing, China) double-beam UV-vis spectrophotometer equipped with a tungsten lamp as the source and 3.5 mL quartz cuvette cells (Fisher Scientific, Waltham, MA, USA). The pH values were recorded by a WTW Inolab 720 pH meter (Weilheim, Germany). The Bruker XRD (Karlsruhe, Germany) was used to study the crystalline nature of the nanocomposite at 40 kV CuKα. The magnetic properties of freshly prepared magnetic nanocomposite (MGO@CdS) were identified with a LakeShore 7400 vibrating sample magnetizer, VSM (Westerville, OH, USA), under a magnetic field of 16.7 Oe. In this regard, 25 mg of adsorbent is fixed in tape, and the field is swiped in vertical mode.

2.3. Synthesis of the Adsorbent

2.3.1. Cadmium Sulfide Nanoparticles

The CdS nanoparticles were prepared simply in a one-step procedure: 10 mL polyethene glycol was added to 10 mmol of cadmium acetate and 10 mmol of sodium thiosulfate. The resulting solution was subjected to mild heat and stirred simultaneously. Then, the mixture was washed (with distilled water) and filtered repeatedly to remove byproducts. Finally, it was oven-dried at 60 °C for 24 h [23].

2.3.2. Synthesis of Graphene Oxide

Graphene oxide was synthesized through the Hummers–Offeman method based on the oxidation of graphite [6,24]. For this purpose, graphite with sodium nitrate, sulfuric acid, and potassium permanganate were blended gradually in the ice bath for 2 h. Next, 100 mL of distilled water was slowly added, whereas the water bath temperature was kept at 35 °C. After 30 min, the solution was placed in a <100 °C water bath, and 5 mL of H_2O_2 was added to the solution until it changed to yellow. For byproduct elimination, washing the product several times with excess distilled water is essential. The resulting mixture was oven-dried at 80 °C for 10 h to produce graphene oxide.

2.3.3. Synthesis of Fe_3O_4@GO

An amount of 0.5 g of $FeCl_3 \cdot 6HO$ and 1 g of $FeCl_3 \cdot 4HO$ (1:2) 1 g of synthesized graphene oxide (GO) were placed in an Erlenmeyer flask, and 50 mL of distilled water was added to it. The obtained solution was subjected to ultrasonic treatment for 30 min. Next, the container was kept in a 50 °C water bath with 2 mL of NH_3 being injected gradually. The solution was filtered and washed with ethanol and water. Finally, Fe_3O_4@GO was dried in the oven at 80 °C for 10 h.

2.3.4. Synthesis of MGO@CdS

The freshly prepared MGO (1 g), 2.6 g cadmium acetate, and 1.58 g sodium thiosulfate were added to 10 mL of polyethene glycol. The solution was stirred and heated at 60 °C for 30 min synchronously to complete the reaction. After washing (with excess distilled water) and oven-drying at 80 °C, the resulting MGO@CdS was employed as sorbent for the MSPE method [25].

2.4. Magnetic Solid Phase Extraction Procedure

The MSPE method based on Fe_3O_4@CdS nanoparticles was used for the extraction of penicillin and tetracycline from human serum samples. The extractions were performed on a solution containing 20 mg of the adsorbent and 60 mL of 0.1 mg L^{-1} analyst. To enhance the adsorption process, the solution was shaken on a circulation shaker at a constant speed of 400 rpm for 40 min at room temperature. Thereafter, the adsorbent was separated from the solution using an external magnet, and the supernatant was decanted. For desorption of the analytes, the adsorbent was agitated in 4 mL of methanol for 5 min at room temperature. Finally, the concentrations of the analytes were determined using a UV-vis spectrophotometer.

3. Results and Discussion

3.1. Characterization

The freshly prepared nanomaterials were characterized using FTIR spectroscopy, EDX, and FESEM. The surface functional groups of the newly synthesized MGO, CdS nanoparticles, and MGO@CdS were investigated by FT-IR. Figure 1A illustrates several intensive FT-IR signals for MGO corresponding to graphene oxide at 3432, 2929, 1726, 1629, 1380, 1215, and 1054 cm^{-1}, which respectively attribute to O–H, C–H, C=O, O–H (bending), C=C, C–O–C (epoxy), and C–OH bands. These are comparable with the FTIR spectra of graphene oxide that were reported previously. As Tan et al. [26] reported that graphite does not possess any functional groups but C=C/C–C at around 1490 cm^{-1}, the

FT-IR spectrum of GO indicates that graphite powder is successfully converted to graphene oxide. The magnetization of graphene oxide can be substantiated by a sharp and intense peak at 549 cm^{-1} (Fe-O). This confirms that Fe$_3$O$_4$ nanoparticles are doped onto graphene oxide (Figure 1A). The synthesis of CdS nanoparticles was also approved by FT-IR spectra (Figure 1B). The characteristic peaks at 638 cm^{-1} ascribe to the Cd–S band [27,28], as well as peaks at 2900 cm^{-1} and 500–600 cm^{-1} are related to S–H stretching and metal-sulfur bonding, respectively [29]. Figure 1C shows the appearance or disappearance of some peaks in the spectrum of MGO@CdS regarding those of MGO (A) and CdS (B), as well as the shifting of peaks at 1731 cm^{-1} (C=O), 1586 cm^{-1} (O–H), 1112 cm^{-1} (C–O), 1005 cm^{-1} (C–OH), and 635 cm^{-1} (Cd-S), which are indicating that CdS nanoparticles were anchored onto the magnetic graphene oxide to produce MGO@CdS nanocomposite.
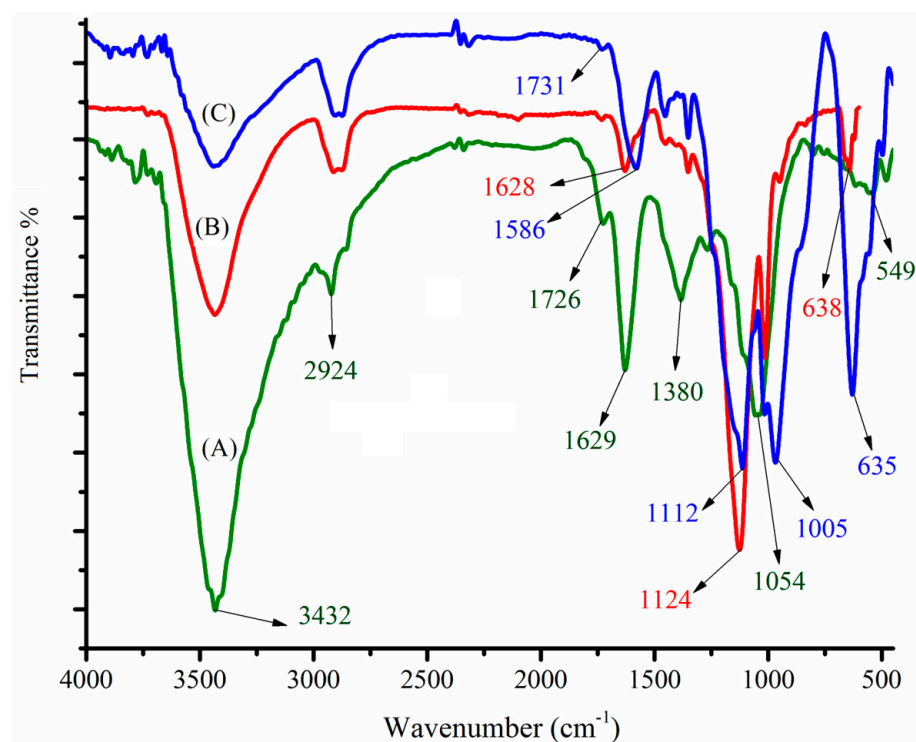

Figure 1. FTIR spectra for (**A**) synthesized MGO, (**B**) CdS nanoparticles, and (**C**) MGO@CdS nanocomposite.

The surface morphology of synthesized nanocomposites was studied with scanning electron microscopy (FESEM). Figure 2A shows the morphology of synthesized CdS nanoparticles, which clearly illustrates the agglomeration of CdS nanoparticles. Figure 2B illustrates a clear observation of the 2D plane of GO sheets. It is also shown that Fe$_3$O$_4$/CdS nanoparticles are well anchored onto the GO plane. These indicate that the GO sheet effectively decreased the aggregation of the nanoparticles.

The distribution of Fe$_3$O$_4$/CdS nanoparticles on GO sheets was characterized using EDX elemental analysis. The EDX spectrum (Figure 2C) confirms the elemental composition of the CdS nanoparticles as O (39%), S (15%), and Cd (44%). Figure 2D shows the existence of C (26.42%), O (32.23%), and Fe (16.45%) elements from graphene oxide and iron oxide. Meanwhile, the presence of Cd (17.38%) and S (7.52%) is evidently from CdS nanoparticles. Hence, such evidence indicates the successful preparation of MGO@CdS nanocomposites.
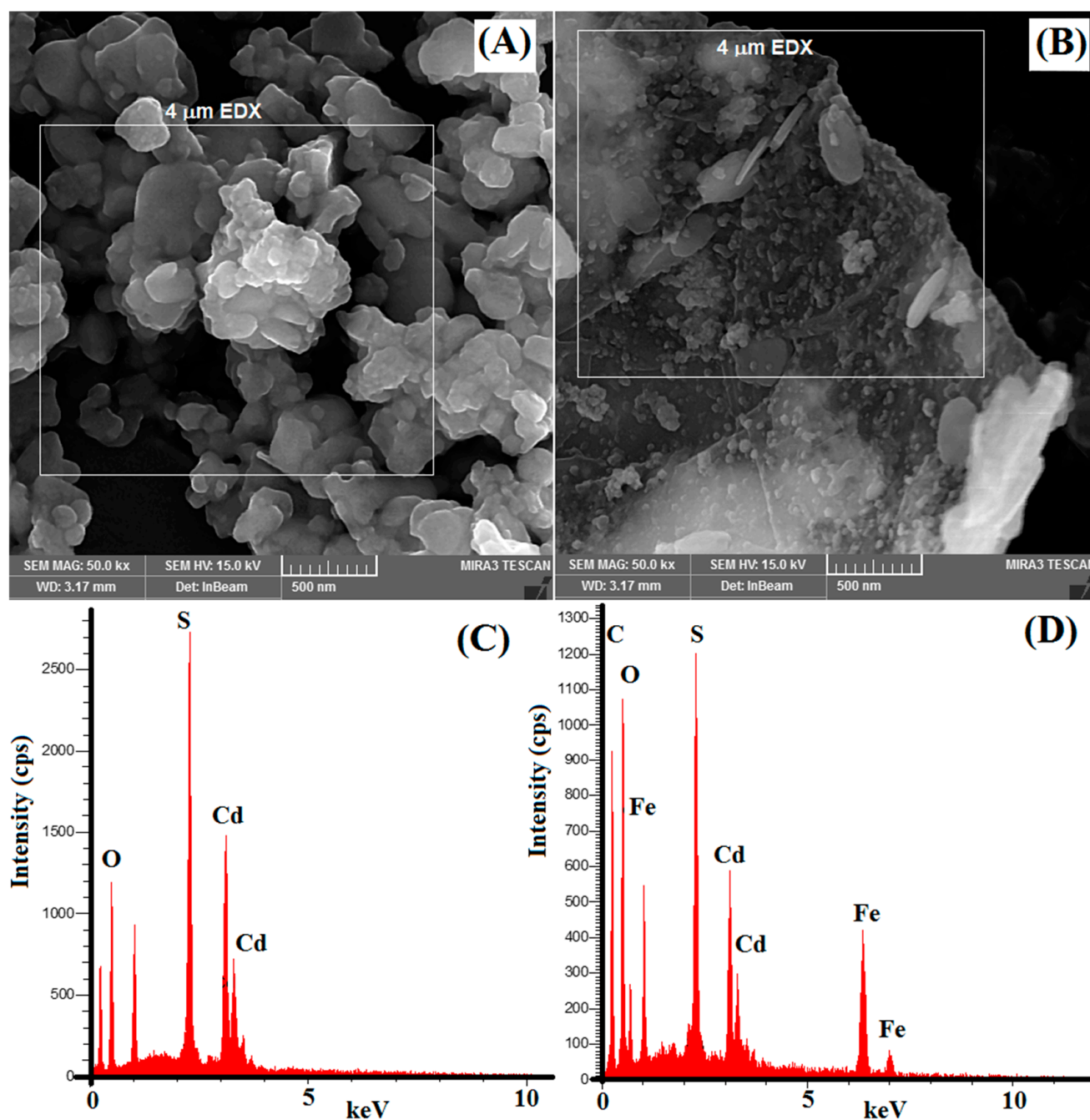
Figure 2. SEM micrograph of (**A**) CdS nanoparticles and (**B**) magnetic MGO@CdS nanocomposite. EDX spectra of (**C**) CdS nanoparticles and (**D**) MGO@CdS nanocomposite (applied voltage for EDX is 20 keV, and the selected area in EDX is shown in micrographs as 4 μm).

The sorbent's magnetic properties play a critical role in the MSPE method because magnetic materials can be collected from aqueous media using an external magnet without filtration or centrifugation. Thus, the magnetic properties of the newly developed adsorbent (MGO@CdS) were investigated with VSM. The magnetic hysteresis curve is from the VSM technique, as shown in Figure 3A. The curve has good magnetic properties for MGO since its magnetization saturation (MS) plateau is observed at ~30 emu/g. It was evident that after adding CdS nanoparticles over MGO, the MS plateau level or magnetic properties did not change significantly. In the case of MS level, ~18 emu/g is well enough to collect the magnetic material in water aqueous media with the assistance of an external magnet.
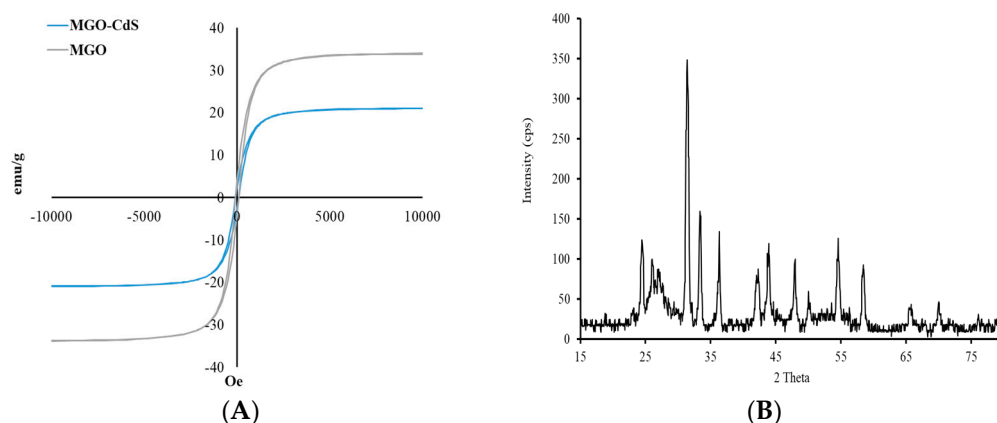
Figure 3. (**A**) Magnetic VSM curve and (**B**) XRD pattern for the MGO@CdS nanocomposite.

The magnetic nanocomposite crystallinity was examined with XRD (Figure 3B). According to the XRD pattern, the signals at 30°, 35°, 42°, 54°, and 64° are performed by the mixture of iron oxide nanoparticles (Fe_2O_3 and Fe_3O_4). The low intensity of the proposed signal is due to the low number of MNPs in the nanocomposite. The sharp signals at 23°, 31°, 33°, 42°, and 48° correspond to the CdS nanoparticles. The broad peak at 24–27° reflects the presence of amorphous graphene oxide.

3.2. Optimization of Key Parameters for Extraction Efficiency

Effective parameters for MSPE performance, namely type of solvent, solvent volume, desorption time, pH, NaCl salt, adsorbent dosage, extraction time, and sample volume, were optimized as follows:

3.2.1. Type of Solvent

The choice of desorption solvent is a significant step in extraction because the extraction efficiency directly depends on the type of solvent [30]. In this work, ethanol, methanol, acetonitrile, basic ethanol, basic methanol, and glycine (with different polarities) were employed for the desorption of selected analytes from the adsorbent. Figure 4A shows that methanol has the most significant performance among the examined solvents, probably due to the higher polarity of methanol, which can overcome the attraction force between adsorbent and analytes [30].

3.2.2. Effect of Eluent Volume

The volume of elution solvent plays an important role in extraction efficiency because it can directly affect the enrichment factor [31]. Thus, different volumes of MeOH (4–10 mL) were examined for desorption of penicillin and tetracycline from the sorbent surface. Based on the obtained data (Figure 4B), maximum extraction efficiency is obtained at 4 and 5 mL for tetracycline and penicillin, respectively. Thereafter, the extraction efficiency decreased, probably due to the dilution effect. Hence, 5 mL was selected as the optimum volume.

3.2.3. Effect of Desorption Time

The desorption time (while the sample solution is shaking) is another important factor in the extraction process that should be taken into account. Therefore, the desorption time was studied in the time range from 1 to 20 min. Figure 4C shows that increasing the time from 1 to 7 min improves the extraction efficiency value for the target analytes. Up to 10–15 min, the value for tetracycline stays almost constant, and that of penicillin also shows no significant change. Afterward, the extraction efficiency decreases noticeably for both analytes. This is probably due to the reactivation of the adsorption sites followed by an increase in the sorption affinity of adsorbent toward the analytes. Thus, 7 min was used as the best desorption time for both analytes.
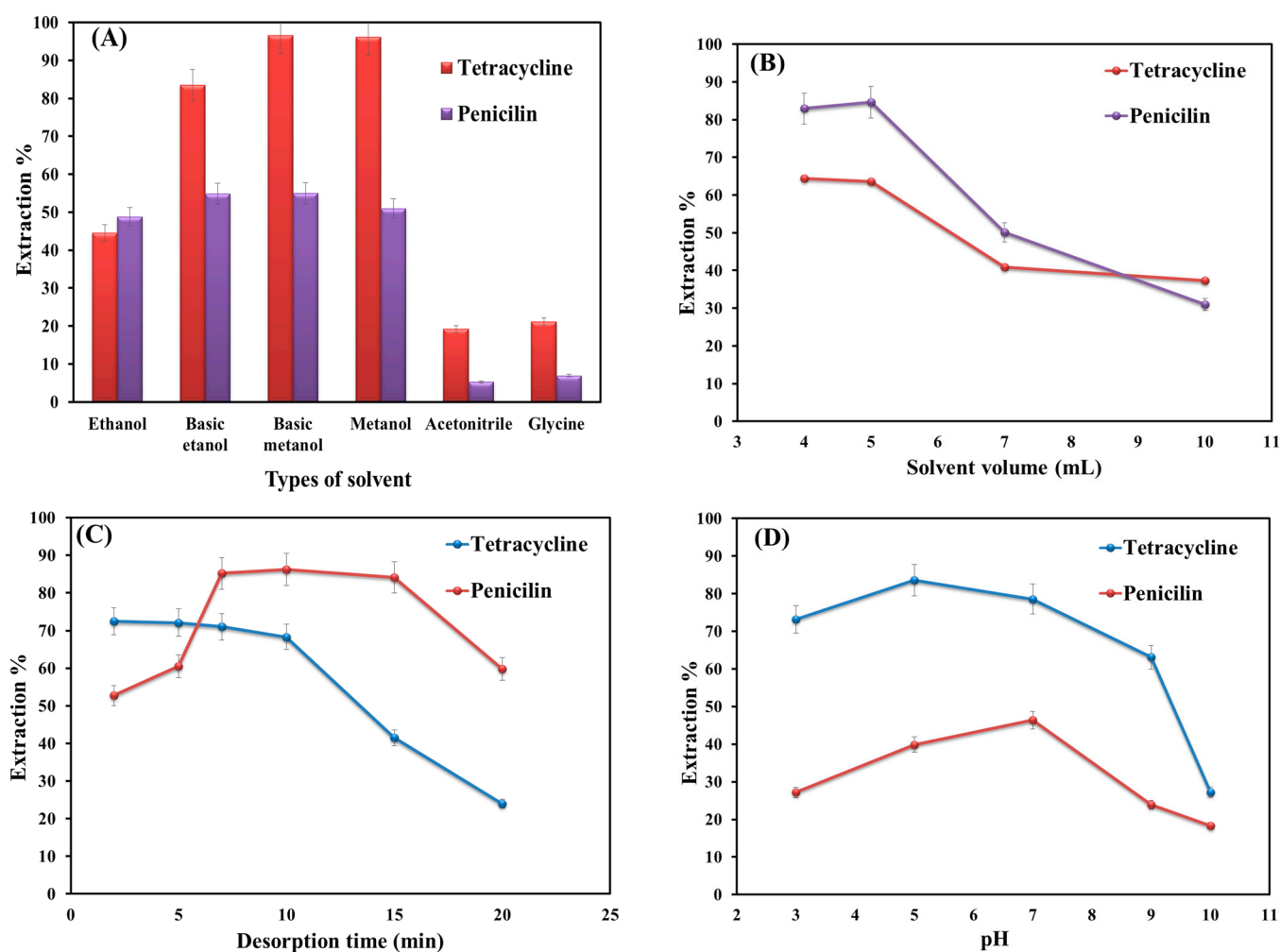
Figure 4. Optimization of key parameters on the extraction efficiency: (**A**) types of solvents; (**B**) volume of selected solvent; (**C**) desorption time; and (**D**) solution pH.

3.2.4. Effect of pH

Solution pH is an important parameter in the extraction process as it changes both the degrees of adsorbent ionization and analyte dissociation [32]. To study the influence of pH on extraction performance, the solution pH was altered from 3 to 10 (Figure 4D). As shown in Figure 4D, the extraction efficiency value of target analytes in an aqueous solution is highly dependent on the solution pH. At low pH (<5) or high ones (>7), the level of extraction decreases significantly. This is probably due to the cleaving of the β-lactam ring in the penicillin structure [33]. At pH levels around 6, penicillin can reach its maximum structural stability. Because at this pH, the penicillin-free energy of decomposition is extremely high [34]. Thus, the extraction of penicillin was conducted in phosphate buffer due to the high stability of penicillin in the buffer. Furthermore, phosphate, as an invisible compound in UV-visible spectroscopy, does not interfere with the experiments [35].

The highest extraction efficiency value for tetracycline is obtained at pH 7. This is because, at low pHs, the amine groups and dissociation constants ($pK_a = 9.7$) give rise to positive net charges. This would cause an increase in the electrostatic attraction between tetracycline and the adsorbent [36]. Furthermore, π-π interactions can form between the benzene ring of tetracycline and graphene oxide sheets. Occurrences of H-bonding and cation-π bonding are also possible. In this light, pH 7 is selected for further experiments.

3.2.5. Salt Addition

The addition of salt can affect the extraction performance by changing the sample solution's ionic strengths and the analytes' solubility [37]. Hence, different NaCl salt contents (0.1 to 10 *w/v*) were added to the aqueous solutions of penicillin and tetracycline to determine the salt effect on extraction efficiency. As shown in Figure 5A, it is clear that the addition of salt up to 2% *w/v* leads to improving the extraction efficiency value. This is due to the increase in the distribution constant between the sample solution and adsorbent and also to the enhancement in the ionic strength. The increase in salinity from 2 to 10% *w/v* does not change the efficiency value significantly. This is probably due to the decrease in mass transfer and diffusion coefficients and the occupation of the adsorbent active sites by excessive salt.
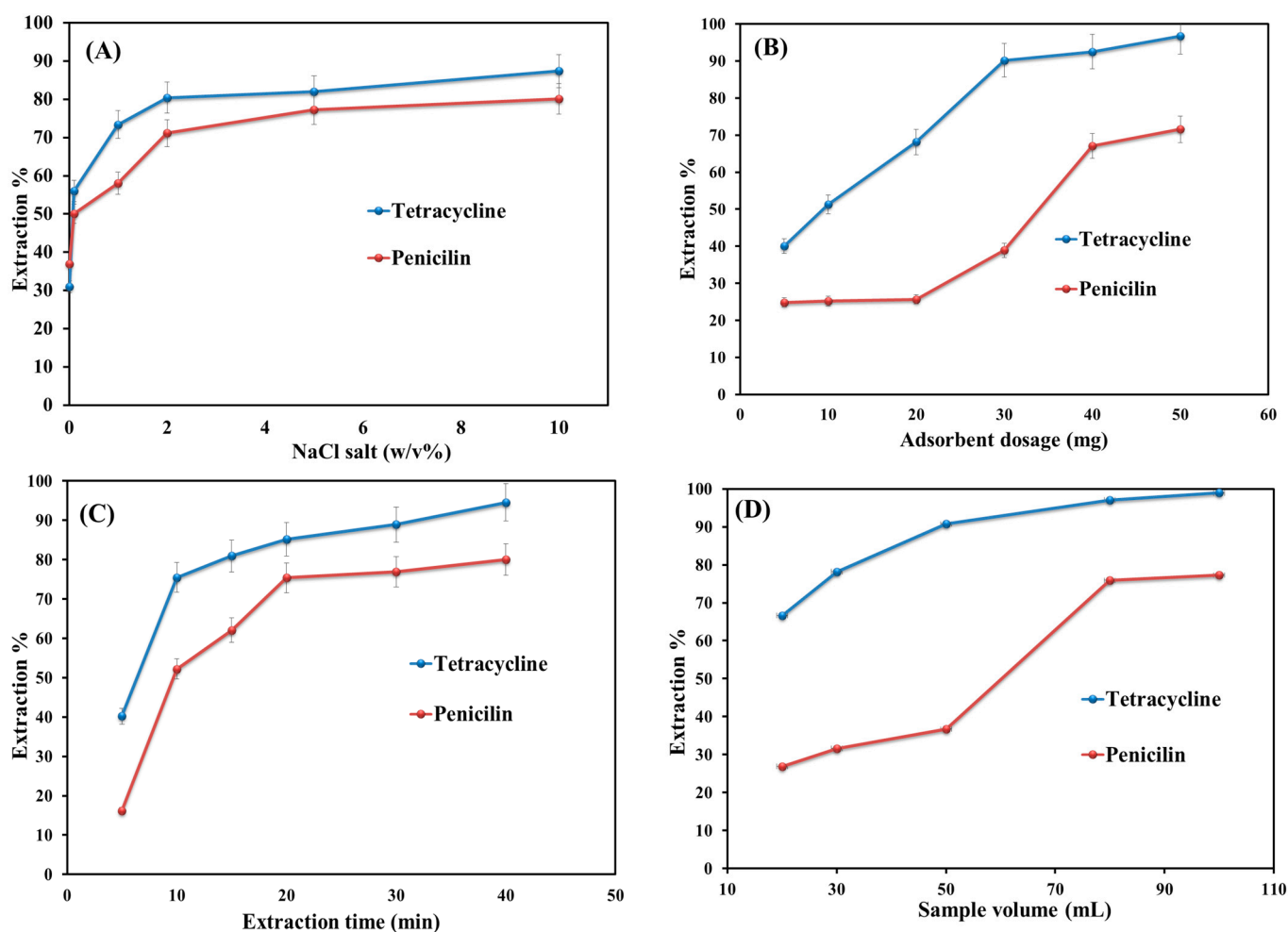

Figure 5. Optimization of key parameters for extraction efficiency: (**A**) salt addition; (**B**) adsorbent dosage; (**C**) extraction time; and (**D**) sample volume.

3.2.6. Effect of Adsorbent Dosage

The quantity of MNPs is an important extraction efficiency metric [3]. The effect of adsorbent dosage on the extraction performance was examined by adding six different amounts (5–50 mg) of adsorbent to the sample solutions (Figure 5B). It indicates that the extraction efficiency value increases with an increase in the amount of adsorbent from 5 to 40 mg. This is because of the availability of more active sites in high dosages [38]. By further increasing the adsorbent amount from 40 to 50 mg, the extraction efficiency did not change significantly and remained slightly constant. This is because of the occupation of the sorption sides by the selected analytes. Hence, 20 mg was selected as the optimum dosage for the adsorbent.

3.2.7. Effect of Extraction Time

The optimized extraction time factor is the required time to guarantee the equilibrium partition (between analytes and adsorbent), high precision, and sensitivity of the method [39]. Thus, shaking time varied from 5 to 40 min (Figure 5C). As shown in Figure 4C, only 20 min are needed to complete the extraction of penicillin and tetracycline from sample solutions. Furthermore, this proposed time indicates the occurrence of a mass transfer process very quickly. Afterward, the extraction efficiency value remains almost constant by increasing the time from 20 to 40 min. Finally, 20 min was obtained as the optimum extraction time.

3.2.8. Sample Volume

Sample volume can impact extraction sensitivity and performance by affecting the enrichment factor and breakthrough volume [40]. Furthermore, by increasing the sample volume, the enrichment factor also increases [41]. The effect of sample volume on extraction efficiency was investigated in the range of 20–100 mL. Figure 5D shows that the extraction efficiency increased by increasing the sample volume from 20 to 80 mL and thereafter remained almost constant up to 100 mL. Hence, 80 mL was selected as the sample volume for further experiments.

3.3. Method Validation

The analytical performance of the proposed MSPE method in the extraction of penicillin and tetracycline was evaluated in terms of the limit of detection (LOD), the limit of quantitation (LOQ), the linear dynamic range (LDR), the determination of coefficient (R^2) and enrichment factor (EF), precision, and reusability under the optimized experimental conditions, and the results are given in Table 1. The calibration curves were constructed using the standard solutions of the analytes at five concentration levels (20–200 µg L^{-1}) of tetracycline and penicillin. The enrichment factor was calculated using Equation (2). The limit of detection was calculated based on $3 \times S_d/m$ (where S_d is the standard deviation of the blank and m is the slope of the calibration graph). The limit of quantitation was obtained with a LOQ of $10 \times S_d/m$. The repeatability and reproducibility of the work examined under intra-day and inter-day precision protocol relative standard deviation (RSD%), which are listed in Table 1.

Table 1. MSPE method validation parameters and precision RSD%.

Compound	Equation	$R^{2\,a}$	LOD [b]	LOQ [c]	LDR [d]	EF [e]	RSD% Intraday	RSD% Interday
Tetracycline	y = 0.6758 × −0.0044	0.997	0.045	0.153	0.02–0.2	20	3.1–4.77	8.41–10.5
Penicillin	y = 0.582 × −0.0008	0.992	0.057	0.191	0.02–0.2	20	3.49–5.8	8.21–12.3

[a] Limit of detection (µg L^{-1}). [b] Limit of quantification (µg L^{-1}). [c] Linear dynamic range (µg L^{-1}). [d] Determination coefficient. [e] Enrichment factor.

The precision of the proposed method was assessed by using intra-day (three analyses, $n = 3$) and inter-day (three days, $n = 9$) experiments. This yielded appropriate RSDs% values for both antibiotics for intraday (3.1–5.8%, $n = 3$) and inter-day (8.2–12.3%, $n = 9$) experiments.

In analytical approaches, the stability of the adsorbent is important because it is highly influential economically. Accordingly, the stability of the newly synthesized MGO@CdS nanocomposite was continuously examined by the extraction of penicillin and tetracycline (0.2 µg L^{-1}) antibiotics from spiked water. After each extraction process, the analytes were washed off the adsorbent using methanol for 10 min. After repeating the extraction 5 times, the percent adsorption values obtained from tetracycline and penicillin were 86.5% and

80.4%, respectively. All parameters' enrichment factor (*EF*) and extraction efficiency (*E%*) are calculated based on Equations (1) and (2), respectively.

$$EF = \left(\frac{C_{found}}{C_{spiked}}\right) \times 100 \tag{1}$$

$$E\% = \left(\frac{C_{found}}{C_{spiked}}\right) \times \left(\frac{V_{eluant}}{V_{sample}}\right) \times 100 \tag{2}$$

where C_{found} is the final concentration of the analytes in eluent (instrument analysis) and C_{spiked} is the initial concentration of analytes in the sample solution.

3.4. Real Sample Analysis

To measure the reliability and applicability of the developed MSPE MGO@CdS for real samples, it was effectively applied to human serum with complex matrices. The serum was spiked with a dosage of 600 units per milliliter of penicillin. The serum samples were analyzed under spiked and unspiked conditions (Table 2). The unspiked experiment was carried out as explained in Section 2.4 without any addition of analytes to the standard solution. The spiked experiment was performed by adding 0.1 μg mL^{-1} (100 μg L^{-1}) of each analyte to 100 mL of serum samples. The proposed procedure was applied to both non-spiked and spiked water samples, and the relative recoveries (*RR%*) were calculated using Equation (3). Extraction recovery values are listed in Table 2 for the triple analysis of tetracycline and penicillin in the serum sample. Hence, appropriate relative recovery values (*RR%*) were obtained for selected antibiotics, ranging from 71% to 110%.

$$RR\% = \left(\frac{C_{extracted} - C_{found}}{C_{spiked}}\right) \times 100 \tag{3}$$

where C_{found}, C_{real}, and C_{added} are the concentrations of analytes in the spiked real sample, the concentration of analytes in the real sample, and the concentration of standard solution added to the real sample, respectively.

Table 2. Results for the extraction of tetracycline and penicillin from human serum using the proposed MSPE method.

Sample	Antibiotics	Spiked (μg L^{-1})	Found (μg L^{-1})	RR%	RSDs%
Human serum	Tetracycline	0.0	nd	—	—
		100	109.5	109.5	7.1
	Penicillin	0.0	1.03	—	—
		100	71.59	71.5	11.6

RR—relative recovery; nd—not detected; RSD—relative standard deviation.

3.5. Antibiotics Release Study

The release of penicillin and tetracycline from MGO@CdS was examined in simulated gastric (pH = 1.2) and intestinal (pH = 7.4) fluids. For this purpose, 100 μg L^{-1} of penicillin and tetracycline were loaded on MGO@CdS. Afterwards, the adsorbent (including loaded analytes) was shaken in simulated gastric and intestinal fluid for 24 h, followed by sampling at scheduled time intervals. Each sample was determined by UV-vis spectrophotometry. Figure 6 shows the releasing profiles of both antibiotics in simulated gastric and intestinal fluids. As can be seen, for 24 h, tetracycline was released more efficiently at pH 1.2 (gastric) compared to its release at pH 7.4 (intestinal). Penicillin-releasing profile at pH 7.4 (intestinal) is more effective than at pH 1.2 (gastric). This is probably due to the β-ring cleavage of penicillin at an acidic pH [33]. Overall, tetracycline was released more effectively than penicillin in both simulated fluids for 24 h. Hence, Figure 6 indicates that both drugs were released slowly. The drug release rate is important in the determination of toxicity and

therapeutic activity [42]. Accordingly, it can be claimed that the synthesized MGO@CdS adsorbent can be used as an efficient material for drug delivery approaches.
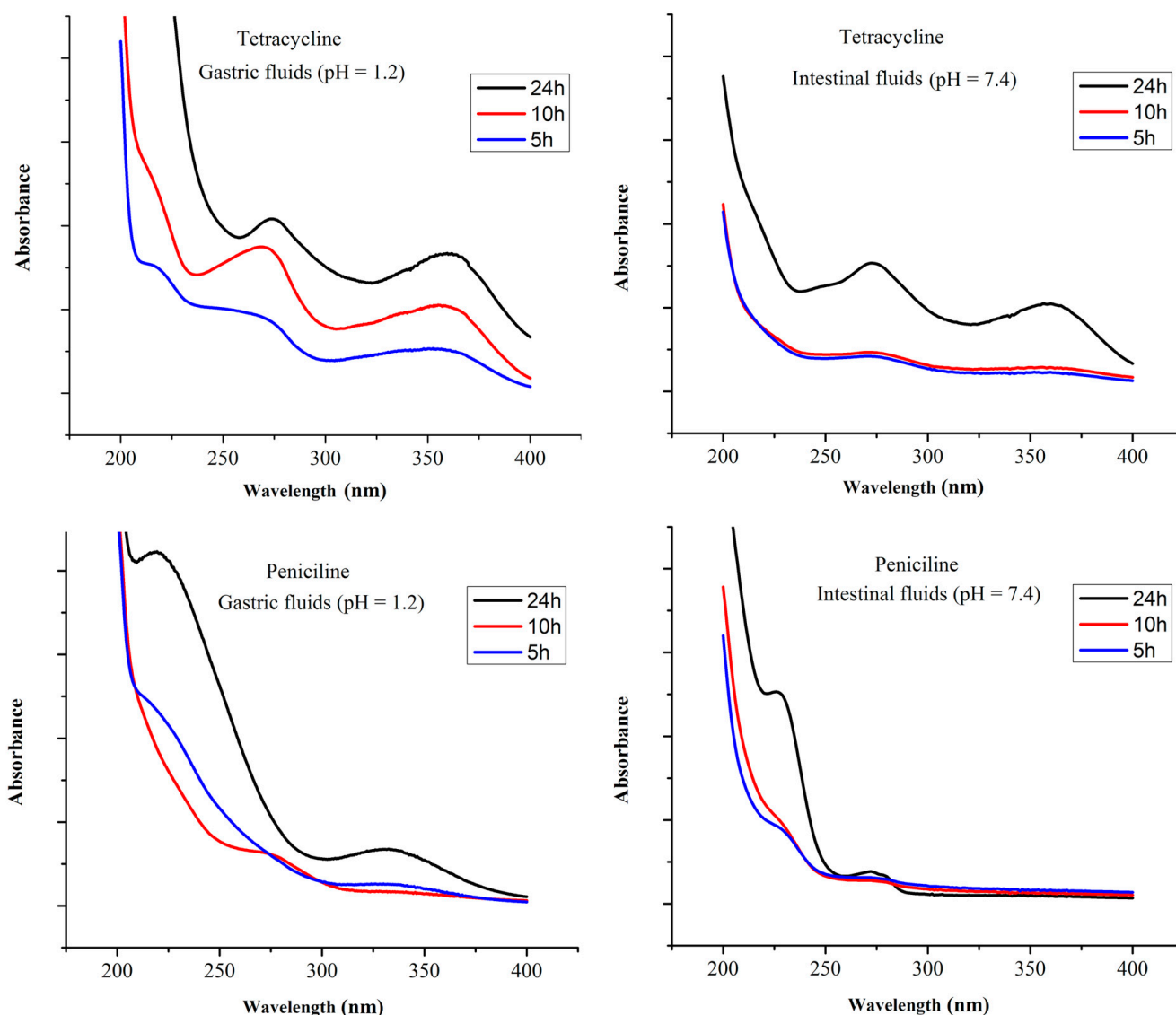

Figure 6. Releasing spectrum of tetracycline and penicillin in body fluids of the gastric and intestinal tract at different times of 5 to 24 h (100 μg L^{-1} of each analyte).

3.6. Comparison with Other Studies

Table 3 shows the comparison study of different adsorbents used to determine different antibiotics in terms of LOD values, extraction methods, and detectors used. The carbon-based adsorbents (OMWCNTs and graphene oxide) provided satisfactory LODs. This is probably due to the presence of π-π interactions between the adsorbent and antibiotics. Furthermore, lower LODs of OMWCNTs and MIP also correspond to a sensitive detector. Hence, MGO@CdS provides a lower LOD value compared with RP-C8 and C18. This is due to the large active sites and hydrophilic nature of MGO@CdS. Nevertheless, this newly synthesized MGO@CdS is comparable with the previously reported adsorbents. However, the MSPE method is faster than SPE and dSPE and also provides appropriate LODs for antibiotics in real samples.

Table 3. Comparison study of the proposed MGO@CdS MSPE with other published materials and methods.

Adsorbent	Analytes	LOD (μg L^{-1})	Method	Analysis	Ref.
MGO@CdS	Tetracycline	0.045	MSPE	UV-vis	This study
	Penicillin	0.056			
OMWCNTs [a]	Quinolone	0.028–0.094	d-SPE [b]	CE-DAD [c]	[43]
Graphene oxide	Tetracycline	0.89	SPE	MALDI-TOF MS [d]	[44]
C18	Tetracycline	1.5–100	SPE	HPLC-DAD	[45]
RP [e]-C8	Tetracycline	31	SPE	HPLC-DAD	[46]
MIP [f]	Tetracycline	0.2	SPE	LC-MS/MS	[47]

[a] Oxide multi-walled carbon nanotube. [b] Dispersive solid phase extraction. [c] Capillary electrophoresis-diode array detector. [d] Matrix-assisted laser desorption/ionization-time of flight mass spectrometry. [e] Reversed phase. [f] Molecularly imprinted polymer.

4. Conclusions

In this study, a novel magnetic graphene oxide-based adsorbent decorated with CdS nanoparticles was successfully synthesized and employed as an appropriate sorbent for the extraction of penicillin and tetracycline from human serum samples. In the cases of penicillin and tetracycline, the adsorption efficiency value is improved by the CdS nanoparticles doped on magnetic graphene oxide. At pH 7, the proposed MSPE methods exhibited acceptable linearity (20–200 μg L^{-1}), sufficient precision, satisfactory repeatability, and a notable enrichment factor (20). Furthermore, it was concluded that the MSPE method based on MGO@CdS provides satisfactory recovery values of 71.47% (for penicillin) and 109.52% (for tetracycline) for human serum samples. The proposed procedure proved to be fast (20 min), simple (two stages), and inexpensive (20 mg of nanoparticles) and was applied as a promising candidate for the determination of antibiotics in human serum samples. The experiments on drug-releasing profiles for penicillin and tetracycline also indicated that the newly synthesized sorbent is suitable for drug-delivery approaches.

Author Contributions: Conceptualization, H.S. and H.R.N.; methodology, H.R.N.; software, E.S.; validation, S.S. (Sara Soltani), E.P. and H.R.N.; formal analysis, S.S. (Sara Soltani); investigation, S.S. (Sara Soltani); resources, E.P.; data curation, N.S.; writing—original draft preparation, E.P.; writing—review and editing, E.P., S.S. (Syed Shahabuddin) and N.S. visualization, E.S.; supervision, H.S., S.S. (Syed Shahabuddin) and N.S.; project administration, H.S.; funding acquisition, S.S. (Syed Shahabuddin) and N.S. All authors have read and agreed to the published version of the manuscript.

Institutional Review Board Statement: Not applicable.

Informed Consent Statement: Not applicable.

Data Availability Statement: Not applicable.

Conflicts of Interest: The authors declare no conflict of interest.

References

1. Adewuyi, A. Chemically Modified Biosorbents and Their Role in the Removal of Emerging Pharmaceutical Waste in the Water System. *Water* **2020**, *12*, 1551. [CrossRef]
2. Mosleh, N.; Najmi, M.; Parandi, E.; Nodeh, H.R.; Vasseghian, Y.; Rezania, S. Magnetic sporopollenin supported polyaniline developed for removal of lead ions from wastewater: Kinetic, isotherm and thermodynamic studies. *Chemosphere* **2022**, *300*, 134461. [CrossRef] [PubMed]

3. Cherkashina, K.; Voznesenskiy, M.; Osmolovskaya, O.; Vakh, C.; Bulatov, A. Effect of surfactant coating of Fe_3O_4 nanoparticles on magnetic dispersive micro-solid phase extraction of tetracyclines from human serum. *Talanta* **2020**, *214*, 120861. [CrossRef] [PubMed]

4. Hunge, Y.M.; Yadav, A.A.; Kang, S.-W.; Kim, H. Photocatalytic degradation of tetracycline antibiotics using hydrothermally synthesized two-dimensional molybdenum disulfide/titanium dioxide composites. *J. Colloid Interface Sci.* **2022**, *606*, 454–463. [CrossRef] [PubMed]

5. Smith, R.A.; M'ikanatha, N.M.; Read, A.F. Antibiotic resistance: A primer and call to action. *Health Commun.* **2015**, *30*, 309–314. [CrossRef]

6. Shirani, M.; Aslani, A.; Sepahi, S.; Parandi, E.; Motamedi, A.; Jahanmard, E.; Nodeh, H.R.; Akbari-Adergani, B. An efficient 3D adsorbent foam based on graphene oxide/AgO nanoparticles for rapid vortex-assisted floating solid phase extraction of bisphenol A in canned food products. *Anal. Methods* **2022**, *14*, 2623–2630. [CrossRef]

7. Otero, L.H.; Rojas-Altuve, A.; Llarrull, L.I.; Carrasco-López, C.; Kumarasiri, M.; Lastochkin, E.; Fishovitz, J.; Dawley, M.; Hesek, D.; Lee, M.; et al. How allosteric control of *Staphylococcus aureus* penicillin binding protein 2a enables methicillin resistance and physiological function. *Proc. Natl. Acad. Sci. USA* **2013**, *110*, 16808–16813. [CrossRef]

8. Arano-Martinez, J.A.; Martínez-González, C.L.; Salazar, M.I.; Torres-Torres, C. A Framework for Biosensors Assisted by Multiphoton Effects and Machine Learning. *Biosensors* **2022**, *12*, 710. [CrossRef]

9. Shirani, M.; Akbari-Adergani, B.; Nodeh, H.R.; Shahabuddin, S. Ultrasonication-facilitated synthesis of functionalized graphene oxide for ultrasound-assisted magnetic dispersive solid-phase extraction of amoxicillin, ampicillin, and penicillin G. *Microchim. Acta* **2020**, *187*, 634. [CrossRef]

10. Moga, A.; Vergara-Barberán, M.; Lerma-García, M.J.; Carrasco-Correa, E.J.; Herrero-Martínez, J.M.; Simó-Alfonso, E.F. Determination of antibiotics in meat samples using analytical methodologies: A review. *Compr. Rev. Food Sci. Food Saf.* **2021**, *20*, 1681–1716. [CrossRef]

11. Shirani, M.; Aslani, A.; Ansari, F.; Parandi, E.; Nodeh, H.R.; Jahanmard, E. Zirconium oxide/titanium oxide nanorod decorated nickel foam as an efficient sorbent in syringe filter based solid-phase extraction of pesticides in some vegetables. *Microchem. J.* **2023**, *189*, 108507. [CrossRef]

12. Shirani, M.; Parandi, E.; Nodeh, H.R.; Akbari-Adergani, B.; Shahdadi, F. Development of a rapid efficient solid-phase microextraction: An overhead rotating flat surface sorbent based 3-D graphene oxide/lanthanum nanoparticles @ Ni foam for separation and determination of sulfonamides in animal-based food products. *Food Chem.* **2022**, *373*, 131421. [CrossRef] [PubMed]

13. Parandi, E.; Pero, M.; Kiani, H. Phase change and crystallization behavior of water in biological systems and innovative freezing processes and methods for evaluating crystallization. *Discov. Food* **2022**, *2*, 6. [CrossRef]

14. Mosleh, N.; Ahranjani, P.J.; Parandi, E.; Nodeh, H.R.; Nawrot, N.; Rezania, S.; Sathishkumar, P. Titanium lanthanum three oxides decorated magnetic graphene oxide for adsorption of lead ions from aqueous media. *Environ. Res.* **2022**, *214*, 113831. [CrossRef]

15. Bidhendi, M.E.; Parandi, E.; Meymand, M.M.; Sereshti, H.; Nodeh, H.R.; Joo, S.-W.; Vasseghian, Y.; Khatir, N.M.; Rezania, S. Removal of lead ions from wastewater using magnesium sulfide nanoparticles caged alginate microbeads. *Environ. Res.* **2023**, *216*, 114416. [CrossRef]

16. Faraji, M.; Shirani, M.; Rashidi-Nodeh, H. The recent advances in magnetic sorbents and their applications. *TrAC Trends Anal. Chem.* **2021**, *141*, 116302. [CrossRef]

17. Safaripour, M.; Parandi, E.; Aghel, B.; Gouran, A.; Saidi, M.; Nodeh, H.R. Optimization of the microreactor-intensified transesterification process using silver titanium oxide nanoparticles decorated magnetic graphene oxide nanocatalyst. *Process Saf. Environ. Prot.* **2023**, *173*, 495–506. [CrossRef]

18. Wei, D.; Wu, S.; Zhu, Y. Magnetic solid phase extraction based on graphene oxide/nanoscale zero-valent iron for the determination of tetracyclines in water and milk by using HPLC-MS/MS. *RSC Adv.* **2017**, *7*, 44578–44586. [CrossRef]

19. Aghel, B.; Gouran, A.; Parandi, E.; Jumeh, B.H.; Nodeh, H.R. Production of biodiesel from high acidity waste cooking oil using nano GO@MgO catalyst in a microreactor. *Renew. Energy* **2022**, *200*, 294–302. [CrossRef]

20. Mohan, H.; Ramalingam, V.; Karthi, N.; Malathidevi, S.; Shin, T.; Venkatachalam, J.; Seralathan, K.-K. Enhanced visible light-driven photocatalytic activity of reduced graphene oxide/cadmium sulfide composite: Methylparaben degradation mechanism and toxicity. *Chemosphere* **2021**, *264*, 128481. [CrossRef]

21. Xu, J.-J.; An, M.; Yang, R.; Tan, Z.; Hao, J.; Cao, J.; Peng, L.-Q.; Cao, W. Determination of Tetracycline Antibiotic Residues in Honey and Milk by Miniaturized Solid Phase Extraction Using Chitosan-Modified Graphitized Multiwalled Carbon Nanotubes. *J. Agric. Food Chem.* **2016**, *64*, 2647–2654. [CrossRef] [PubMed]

22. Wang, R.; Li, C.; Li, Q.; Zhang, S.; Lv, F.; Yan, Z. Electrospinning fabrication of covalent organic framework composite nanofibers for pipette tip solid phase extraction of tetracycline antibiotics in grass carp and duck. *J. Chromatogr. A* **2020**, *1622*, 461098. [CrossRef] [PubMed]

23. Jume, B.H.; Dana, N.V.; Rastin, M.; Parandi, E.; Darajeh, N.; Rezania, S. Sulfur-Doped Binary Layered Metal Oxides Incorporated on Pomegranate Peel-Derived Activated Carbon for Removal of Heavy Metal Ions. *Molecules* **2022**, *27*, 8841. [CrossRef] [PubMed]

24. Parandi, E.; Safaripour, M.; Mosleh, N.; Saidi, M.; Nodeh, H.R.; Oryani, B.; Rezania, S. Lipase enzyme immobilized over magnetic titanium graphene oxide as catalyst for biodiesel synthesis from waste cooking oil. *Biomass Bioenergy* **2023**, *173*, 106794. [CrossRef]

25. Parandi, E.; Safaripour, M.; Abdellattif, M.H.; Saidi, M.; Bozorgian, A.; Nodeh, H.R.; Rezania, S. Biodiesel production from waste cooking oil using a novel biocatalyst of lipase enzyme immobilized magnetic nanocomposite. *Fuel* **2022**, *313*, 123057. [CrossRef]

26. Tan, L.; Zhang, L.; Sun, Q.; Shen, M.; Qu, Q.; Zheng, H. Capacity loss induced by lithium deposition at graphite anode for LiFePO4/graphite cell cycling at different temperatures. *Electrochimica Acta* **2013**, *111*, 802–808. [CrossRef]

27. Ch, A.; Rao, V.; Ch, S.C. Structural properties of CdS nano particles prepared in the presence of organic solvent. *Appl. Sci. Res.* **2014**, *5*, 99–105.

28. Pourjavaher, S.; Almasi, H.; Meshkini, S.; Pirsa, S.; Parandi, E. Development of a colorimetric pH indicator based on bacterial cellulose nanofibers and red cabbage (*Brassica oleraceae*) extract. *Carbohydr. Polym.* **2017**, *156*, 193–201. [CrossRef]

29. Kim, Y.-Y.; Walsh, D. Metal sulfide nanoparticles synthesized via enzyme treatment of biopolymer stabilized nanosuspensions. *Nanoscale* **2010**, *2*, 240–247. [CrossRef]

30. Korrani, Z.S.; Ibrahim, W.A.W.; Nodeh, H.R.; Aboul-Enein, H.Y.; Sanagi, M.M. Simultaneous preconcentration of polar and non-polar organophosphorus pesticides from water samples by using a new sorbent based on mesoporous silica. *J. Sep. Sci.* **2016**, *39*, 1144–1151. [CrossRef]

31. Nodeh, H.R.; Ibrahim, W.A.W.; Kamboh, M.A.; Sanagi, M.M. Dispersive graphene-based silica coated magnetic nanoparticles as a new adsorbent for preconcentration of chlorinated pesticides from environmental water. *RSC Adv.* **2015**, *5*, 76424–76434. [CrossRef]

32. Nodeh, H.R.; Ibrahim, W.A.W.; Kamboh, M.A.; Sanagi, M.M. New magnetic graphene-based inorganic–organic sol-gel hybrid nanocomposite for simultaneous analysis of polar and non-polar organophosphorus pesticides from water samples using solid-phase extraction. *Chemosphere* **2017**, *166*, 21–30. [CrossRef] [PubMed]

33. Suplatov, D.; Panin, N.; Kirilin, E.; Shcherbakova, T.; Kudryavtsev, P.; Švedas, V. Computational design of a pH stable enzyme: Understanding molecular mechanism of penicillin acylase's adaptation to alkaline conditions. *PLoS ONE* **2014**, *9*, e100643. [CrossRef] [PubMed]

34. El-Sonbati, A.Z.; Diab, M.A.; Morgan, S.M. Thermal properties, antimicrobial activity and DNA binding of Ni(II) complexes of azo dye compounds. *J. Mol. Liq.* **2017**, *225*, 195–206. [CrossRef]

35. Balci, H.; Ozturk, M.T.; Pijning, T.; Ozturk, S.I.; Gumusel, F. Improved activity and pH stability of *E. coli* ATCC 11105 penicillin acylase by error-prone PCR. *Appl. Microbiol. Biotechnol.* **2014**, *98*, 4467–4477. [CrossRef]

36. Nodeh, H.R.; Sereshti, H. Synthesis of magnetic graphene oxide doped with strontium titanium trioxide nanoparticles as a nanocomposite for the removal of antibiotics from aqueous media. *RSC Adv.* **2016**, *6*, 89953–89965. [CrossRef]

37. Eskandarpour, N.; Sereshti, H.; Najarzadekan, H.; Gaikani, H. Polyurethane/polystyrene-silica electrospun nanofibrous composite for the headspace solid-phase microextraction of chlorophenols coupled with gas chromatography. *J. Sep. Sci.* **2016**, *39*, 4637–4644. [CrossRef]

38. Shan, R.-R.; Yan, L.-G.; Yang, K.; Yu, S.-J.; Hao, Y.-F.; Yu, H.-Q.; Du, B. Magnetic Fe₃O₄/MgAl-LDH composite for effective removal of three red dyes from aqueous solution. *Chem. Eng. J.* **2014**, *252*, 38–46. [CrossRef]

39. Asgharinezhad, A.A.; Ebrahimzadeh, H.; Mirbabaei, F.; Mollazadeh, N.; Shekari, N. Dispersive micro-solid-phase extraction of benzodiazepines from biological fluids based on polyaniline/magnetic nanoparticles composite. *Anal. Chim. Acta* **2014**, *844*, 80–89. [CrossRef]

40. Peng, H.; Zhang, N.; He, M.; Chen, B.; Hu, B. Simultaneous speciation analysis of inorganic arsenic, chromium and selenium in environmental waters by 3-(2-aminoethylamino) propyltrimethoxysilane modified multi-wall carbon nanotubes packed microcolumn solid phase extraction and ICP-MS. *Talanta* **2015**, *131*, 266–272. [CrossRef]

41. Zhou, Q.; Lei, M.; Wu, Y.; Yuan, Y. Magnetic solid phase extraction of typical polycyclic aromatic hydrocarbons from environmental water samples with metal organic framework MIL-101 (Cr) modified zero valent iron nano-particles. *J. Chromatogr. A* **2017**, *1487*, 22–29. [CrossRef] [PubMed]

42. Charrois, G.J.R.; Allen, T.M. Drug release rate influences the pharmacokinetics, biodistribution, therapeutic activity, and toxicity of pegylated liposomal doxorubicin formulations in murine breast cancer. *Biochim. Biophys. Acta (BBA) Biomembr.* **2004**, *1663*, 167–177. [CrossRef]

43. Herrera-Herrera, A.V.; Ravelo-Pérez, L.M.; Hernández-Borges, J.; Afonso, M.M.; Palenzuela, J.A.; Rodríguez-Delgado, M. Oxidized multi-walled carbon nanotubes for the dispersive solid-phase extraction of quinolone antibiotics from water samples using capillary electrophoresis and large volume sample stacking with polarity switching. *J. Chromatogr. A* **2011**, *1218*, 5352–5361. [CrossRef] [PubMed]

44. Liu, J.; Liu, Y.; Gao, M.; Zhang, X. High Throughput Detection of Tetracycline Residues in Milk Using Graphene or Graphene Oxide as MALDI-TOF MS Matrix. *J. Am. Soc. Mass Spectrom.* **2012**, *23*, 1424–1427. [CrossRef] [PubMed]

45. Babić, S.; Ašperger, D.; Mutavdžić, D.; Horvat, A.J.; Kaštelan-Macan, M. Solid phase extraction and HPLC determination of veterinary pharmaceuticals in wastewater. *Talanta* **2006**, *70*, 732–738. [CrossRef] [PubMed]

46. HPLC-Photodiode, E.B.M. A simple multi-residue method for determination of oxytetracycline, tetracycline and chlortetracycline in export buffalo meat by HPLC-photodiode array detector. *J. Food Drug Anal.* **2007**, *15*, 278–284.

47. Chen, L.; Liu, J.; Zeng, Q.; Wang, H.; Yu, A.; Zhang, H.; Ding, L. Preparation of magnetic molecularly imprinted polymer for the separation of tetracycline antibiotics from egg and tissue samples. *J. Chromatogr. A* **2009**, *1216*, 3710–3719. [CrossRef]